

III. Radial Diffusion

III.1 Violation of the Third Invariant

Whereas pitch-angle diffusion is customarily invoked as a loss mechanism for the radiation belts, diffusion in Φ is usually associated with creation of the belts. This is especially true of radial diffusion in which M and J are conserved, since particles then gain energy in the process of diffusing toward the earth from an external source (see below). Diffusion in Φ (radial diffusion) at constant M and J thus plays the dual role of injecting particles into the magnetospheric interior and accelerating the particles thereby injected to the energies observed.

In addition to particles that have entered from interplanetary space (and perhaps from the geomagnetic tail), the magnetosphere also contains protons and electrons born internally through the decay of albedo neutrons ejected from the upper atmosphere by energetic (≥ 100 MeV) solar protons and galactic cosmic-ray particles colliding inelastically (in the nuclear sense) with gas atoms. These internal source mechanisms are known as SPAND and CRAND, respectively, for *solar-proton* (and *cosmic-ray*) *albedo neutron decay*. These sources (CRAND is about ten times as intense a particle source as SPAND) typically account for the presence of energetic protons and electrons in the inner zone, but radial diffusion plays an essential role in bringing about the observed spatial and spectral distribution of these particles [38]. In addition, radiation-belt particles may possibly experience *in situ* acceleration to high energies [44] through the absorption of plasma-wave energy. Such an event might easily be interpreted as an "injection" of the energetic particles into the magnetospheric interior (see Section IV.6).

Artificial radiation belts created by high-altitude nuclear detonations (1958—1963) once contributed substantially to the inner-zone particle population. These artificial belts, which had decayed to an intensity below that of the natural radiation by the year 1968, yielded some of the earliest measurements of a radial-diffusion coefficient for radiation-belt electrons in the magnetosphere.

In the outer zone, radial diffusion plays an all-important role in maintaining the level of trapped radiation. Direct observational evidence for the occurrence of third-invariant violation in the outer zone is shown in Fig. 23, which is a tracing of data obtained by instruments

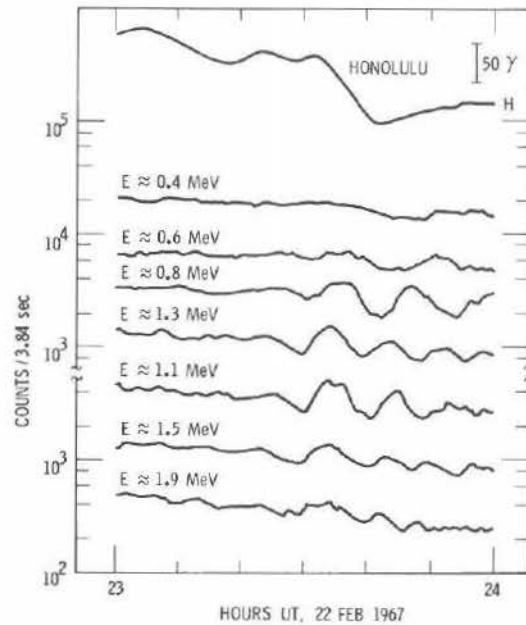


Fig. 23. Drift-periodic echoes in outer-zone electron fluxes, as observed on ATS 1 following a negative magnetic impulse [55] at 2330 UT (1330 LT).

on the geosynchronous equatorial satellite ATS 1 (longitude 150° W), together with the magnetogram (horizontal, or H , component) for the same time period (1300—1400 local time) from the ground-based station at Honolulu. The interpretation of Fig. 23 is that a negative magnetic impulse, presumably caused by a sudden decrease in solar-wind pressure at the magnetopause, propagates inward from the magnetopause and arrives at Honolulu several minutes after encountering the spacecraft²⁰. Upon arrival at synchronous altitude, the impulse causes a simultaneous decrease of the electron flux observed in each of the seven energy channels. As time goes on, however, particles near the satellite at the arrival time of the impulse drift toward the night side, and electrons from the night side (where the negative impulse was less severe) drift to the azimuthal position of the satellite. This accounts for the recovery of the fluxes in each channel on a time scale of half the energy-dependent drift period. The relative minimum in flux recurs with the return (to the day side) of those particles most severely influenced by the impulse.

²⁰This delay time is in accord with the time required for a rarefactional (magnetosonic) impulse to travel the required distance of 5.6 earth radii at approximately the Alfvén speed.

These *drift-periodic echoes* in the outer-zone electron flux persist well after the passage of the magnetic impulse initiating them. Moreover, the fact that each energy channel “oscillates” at its own characteristic drift frequency is convincing evidence for drift-phase organization of the particles, which therefore (*cf.* Section II.1) have been dispersed with respect to $|\Phi|$ ($\equiv 2\pi a^2 B_0/L$)²¹. The nonvanishing energy bandwidth of each detection channel corresponds to a drift-frequency bandwidth that thoroughly phase-mixes the observations on a time scale of three or four drift periods. Particles initially differing in both φ_3 and energy retain their separate identities, but the detectors can no longer distinguish among them.

The practical fact of phase mixing, and the fact that consecutive sudden impulses are statistically uncorrelated on the drift time scale, provide the essential degree of randomness that makes it appropriate to speak of third-invariant violation in terms of diffusion with respect to Φ . At constant M and J , *i.e.*, with pitch-angle diffusion neglected, the radial-diffusion equation

$$\frac{\partial \bar{f}}{\partial t} = \frac{\partial}{\partial \Phi} \left[D_{\Phi\Phi} \frac{\partial \bar{f}}{\partial \Phi} \right] = L^2 \frac{\partial}{\partial L} \left[\frac{1}{L^2} D_{LL} \frac{\partial \bar{f}}{\partial L} \right] \quad (3.01)$$

follows directly from (2.01), since $D_{LL} \equiv (dL/d\Phi)^2 D_{\Phi\Phi}$. The distribution function \bar{f} is equal to \bar{J}_\perp/p^2 , evaluated on a surface generated by the mirror points of ions or electrons having in common their values of M and J .

In a dipole field this surface coincides with the equatorial plane ($\theta = \pi/2$) for particles having $J=0$. For $J \neq 0$ the mirror-point surface satisfies the equation

$$[y/Y(y)]^2 = 8m_0 B_0 a^2 (M/J^2 L) \equiv B_0 a^2 / K^2 L, \quad (3.02)$$

where y is related by (1.25) to the mirror colatitude θ_m . With the aid of (3.02) and (1.31), the variation of y with L at constant M and J is plotted in Fig. 24 for selected values of y_7 (the value of y at $L=7$). The $L=7$ shell is often used as a reference location in radiation-belt theory because it is quite near the outer boundary of stable trapping, and therefore adjacent to a possibly important source of moderately energetic particles (*i.e.*, solar cosmic rays that have entered the magnetosphere). A secondary reason for the popularity of $L=7$ as a reference shell [40] is that an equatorially mirroring particle's nonrelativistic

²¹This follows from Liouville's theorem, since $J_3/2\pi$ ($\equiv q\Phi/2\pi c$) is canonically conjugate to the drift phase φ_3 .

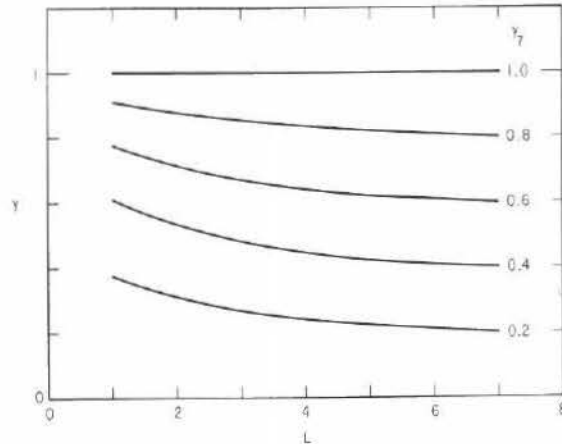


Fig. 24. Systematic variation of y (sine of equatorial pitch angle) with L at constant M and J , applicable to radial diffusion caused by magnetospheric impulses.

kinetic energy $p^2/2m_0$ (measured in keV) at $L=7$ roughly approximates the particle's first invariant M (measured in MeV/gauss).

Except at the end-points $y=0$ and $y=1$, there is a systematic inverse variation (not proportionality) between y and L during radial diffusion at constant M and J . This variation does not constitute pitch-angle diffusion, but rather is an interesting property incidental to radial diffusion. The change in particle energy during diffusion in L can be deduced from the identity $p^2 = 2m_0 MB_0/L^3 y^2$ if $0 < y \leq 1$, or from $p = J/2LaY(y)$ if $0 \leq y < 1$. It follows that p^2 varies more strongly than L^{-2} , but more weakly than L^{-3} , in the interval $0 < y < 1$.

The type of radial diffusion that conserves both M and J [58] can be caused by magnetic sudden impulses (as illustrated in Fig. 23), by substorm-associated impulses of the convection electrostatic field, and by other magnetospheric disturbances operating on a similar time scale (~ 100 sec). In each case the affected particles yield a bounce-averaged response, since the rise time of the impulse (~ 100 sec) is typically much longer than $2\pi/\Omega_2$ (~ 1 sec). On the other hand, the drift periods of many radiation-belt particles (~ 500 sec in Fig. 23) are not extremely long compared to the rise time of a typical sudden impulse, and so a frequency-spectral treatment of impulses is definitely in order. In such a treatment, a particle responds resonantly to Fourier components located at harmonics (including the fundamental) of its drift frequency, although the impulses themselves are hardly oscillatory in character.

In addition to the type of radial diffusion that conserves both M and J , it is possible to conceive of mechanisms that fail to preserve

the first two invariants while violating Φ . Such mechanisms may involve particle collisions or bounce- and cyclotron-resonant interactions with magnetospheric waves. Radial diffusion mechanisms that violate M and/or J often lack the ability to energize particles efficiently in the process, and they generally play a less certain role than sudden impulses in the overall picture of radiation-belt dynamics.

III.2 Magnetic Impulses

In the magnetic-field model specified by (1.45), sudden impulses in \mathbf{B} correspond to sudden changes in b , the geocentric stand-off distance to the subsolar point on the magnetopause. The stand-off distance b is governed, according to (1.43), by the momentum flux of the solar wind. An encounter with the plasma ejected by a solar flare, for example, can lead to a sudden contraction and/or expansion of the magnetosphere. A decrease in b that is sudden on the drift time scale represents a sudden contraction of the magnetosphere. This contraction consists of both an azimuthally symmetric compression of \mathbf{B} (the B_1 term) and an azimuthally asymmetric distortion of \mathbf{B} (the B_2 term). The symmetrical compression, which is easily identified from the magnetograms of ground based ($r=a$) observatories, is adiabatic to the trapped particles. All drift phases φ_3 respond identically to the symmetric part of the sudden impulse, and so this part is reversible. It conserves Φ and produces no radial diffusion.

Induced Electric Field. The accompanying asymmetric distortion (the B_2 term) is not easily distinguished at $r=a$, where it is small in magnitude. However, this part of the impulse does violate the third invariant, thereby producing drift echoes (Fig. 23) and radial diffusion. A sudden impulse in \mathbf{B} affects the geomagnetically trapped particles by virtue of an induced electric field \mathbf{E} , which may be calculated term by term from a field expansion [29] of the form [cf. (1.46)]

$$E_r(r, \theta, \varphi; t) = \sum_{lmn} E_r(l, m, n; t)(r/b)^n \sin^l \theta \sin m\varphi \quad (3.03a)$$

$$E_\theta(r, \theta, \varphi; t) = \sum_{lmn} E_\theta(l, m, n; t)(r/b)^n \cos \theta \sin^l \theta \sin m\varphi \quad (3.03b)$$

$$E_\varphi(r, \theta, \varphi; t) = \sum_{lmn} E_\varphi(l, m, n; t)(r/b)^n \sin^l \theta \cos m\varphi. \quad (3.03c)$$

If the Maxwell relation $c\nabla \times \mathbf{E} = -(\partial \mathbf{B}/\partial t)$, written out in its three components, is applied to (1.46) and (3.03), the time-dependent (but position-independent) coefficients of $[(r/b)^n \sin^{l+1} \theta \cos m\varphi]$ and $[(r/b)^n \cos \theta$

$\times \sin^l \theta \sin m \varphi]$ can be isolated to yield the relationships

$$(n+1)E_\varphi(l, m, n; t) = mE_r(l+1, m, n; t) + (a/c)(b/a)^n \dot{B}_\theta(l, m, n-1; t) \quad (3.04a)$$

$$(n+1)E_\theta(l, m, n; t) = (l+1)E_r(l+1, m, n; t) - (a/c)(b/a)^n \dot{B}_\varphi(l, m, n-1; t), \quad (3.04b)$$

where $\dot{\mathbf{B}} = \partial \mathbf{B} / \partial t$. The third component of $c \nabla \times \mathbf{E} = -(\partial \mathbf{B} / \partial t)$ is redundant, since $\nabla \cdot \mathbf{B} = 0$.

One more condition on \mathbf{E} must be specified in order to solve (3.04). It is customary to state this subsidiary condition as $\mathbf{E} \cdot \mathbf{B} = 0$ [32]. Such a statement is usually justified by an appeal to the cold plasma which is assumed to fill the magnetosphere. The cold plasma serves to short-circuit each field line, in which case the impulsively expanding ($db/dt > 0$) or contracting ($db/dt < 0$) magnetospheric medium is governed by the laws of magnetohydrodynamics (MHD). Since the impulse therefore propagates through the magnetosphere at approximately the Alfvén speed, the field model summarized by (1.46) admittedly violates the principle of causality on time scales shorter than $\sim b/c_A$. For drift periods exceeding a few minutes, however, the arrival time of the impulse at any L shell is *practically* independent of φ_3 , and this condition permits the simplified (instantaneous-response) model to be used for the time-varying \mathbf{B} field.

For the magnetic-field model given by (1.48), application of $\mathbf{E} \cdot \mathbf{B} = 0$ to (3.04) yields the recursion relation [29]

$$\begin{aligned} & [(2n+l+2)/(n+1)] E_r(l, m, n; t) \\ &= (B_1/B_0) [(n-l-2)/(n-2)] E_r(l, m, n-3; t) \\ &+ (B_2/B_0) [(l-n+2)/(n-3)] E_r(l-1, m-1, n-4; t) \\ &+ (B_2/B_0) [(l-n-2)/(n-3)] E_r(l-1, m+1, n-4; t) \\ &- (B_2/2B_0) [(l-m+2)/(n-3)] E_r(l+1, m-1, n-4; t) \\ &- B_2/2B_0 [(l+m+2)/(n-3)] E_r(l+1, m+1, n-4; t) \quad (3.05) \\ &- (4/3c) B_2 (a/b)^3 (db/dt) \delta_{l1} \delta_{m1} \delta_{n2} \\ &+ (1/6c) B_2 (B_1/B_0) (a/b)^3 (db/dt) \delta_{l1} \delta_{m1} \delta_{n5}, \end{aligned}$$

where the Kronecker symbol δ_{ij} is equal to unity (rather than zero) only if $i=j$. Closure of the recursion formula is achieved by requiring that the \mathbf{E} induced by db/dt remain finite in the limit $r=0$. This requirement forces $E_r(l, m, n; t)$ to vanish if $n < 0$. From this starting point it is possible to generate all the coefficients $E_r(l, m, n; t)$ by means of (3.05). The nonvanishing $E_r(l, m, n; t)$ of lowest order n is $E_r(1, 1, 2; t) = -(4/7c)(a/b)^3 (db/dt) B_2$.

The recursion relation yields definite algebraic values for several coefficients which have $m=0$, and which therefore ostensibly can have no physical significance [see (3.03a)]. Such coefficients that multiply zero (in the form of $\sin m \varphi$) are ignored. A correct implementation of (3.05) thus leads to a unique set of electric-field coefficients $E_r(l, m, n; t)$, where $m > 0$, from which $E_\theta(l, m, n; t)$ and $E_\varphi(l, m, n; t)$ are obtainable by means of (3.04). All nonvanishing electric-field coefficients for which $n \leq 10$ are listed in Table 7.

Table 7. Electric-Field Coefficients

$E_r(1, 1, 2; t) = -(4/7)B_2(a^3 \dot{b}/b^3 c)$
$E_r(1, 1, 5; t) = -(9/91)(B_1/B_0)B_2(a^3 \dot{b}/b^3 c)$
$E_r(2, 2, 6; t) = (1/6)(B_2/B_0)B_2(a^3 \dot{b}/b^3 c)$
$E_r(1, 1, 8; t) = -(135/3458)(B_1/B_0)^2 B_2(a^3 \dot{b}/b^3 c)$
$E_r(2, 2, 9; t) = (25/273)(B_2/B_0)^2 B_1(a^3 \dot{b}/b^3 c)$
$E_r(1, 1, 10; t) = -(11/483)(B_2/B_0)^2 B_2(a^3 \dot{b}/b^3 c)$
$E_r(3, 1, 10; t) = -(11/210)(B_2/B_0)^2 B_2(a^3 \dot{b}/b^3 c)$
$E_r(3, 3, 10; t) = -(11/210)(B_2/B_0)^2 B_2(a^3 \dot{b}/b^3 c)$
$E_\theta(0, 1, 2; t) = (8/7)B_2(a^3 \dot{b}/b^3 c)$
$E_\theta(0, 1, 5; t) = -(3/182)(B_1/B_0)B_2(a^3 \dot{b}/b^3 c)$
$E_\theta(1, 2, 6; t) = (1/21)(B_2/B_0)B_2(a^3 \dot{b}/b^3 c)$
$E_\theta(0, 1, 8; t) = -(15/3458)(B_1/B_0)^2 B_2(a^3 \dot{b}/b^3 c)$
$E_\theta(1, 2, 9; t) = (5/273)(B_2/B_0)^2 B_1(a^3 \dot{b}/b^3 c)$
$E_\theta(0, 1, 10; t) = -(1/483)(B_2/B_0)^2 B_2(a^3 \dot{b}/b^3 c)$
$E_\theta(2, 1, 10; t) = -(1/70)(B_2/B_0)^2 B_2(a^3 \dot{b}/b^3 c)$
$E_\theta(2, 3, 10; t) = -(1/70)(B_2/B_0)^2 B_2(a^3 \dot{b}/b^3 c)$
$E_\varphi(1, 0, 1; t) = (3/2)B_1(a^3 \dot{b}/b^3 c)$
$E_\varphi(0, 1, 2; t) = (8/7)B_2(a^3 \dot{b}/b^3 c)$
$E_\varphi(2, 1, 2; t) = -(8/3)B_2(a^3 \dot{b}/b^3 c)$
$E_\varphi(0, 1, 5; t) = -(3/182)(B_1/B_0)B_2(a^3 \dot{b}/b^3 c)$
$E_\varphi(1, 2, 6; t) = (1/21)(B_2/B_0)B_2(a^3 \dot{b}/b^3 c)$
$E_\varphi(0, 1, 8; t) = -(15/3458)(B_1/B_0)^2 B_2(a^3 \dot{b}/b^3 c)$
$E_\varphi(1, 2, 9; t) = (5/273)(B_2/B_0)^2 B_1(a^3 \dot{b}/b^3 c)$
$E_\varphi(0, 1, 10; t) = -(1/483)(B_2/B_0)^2 B_2(a^3 \dot{b}/b^3 c)$
$E_\varphi(2, 1, 10; t) = -(1/70)(B_2/B_0)^2 B_2(a^3 \dot{b}/b^3 c)$
$E_\varphi(2, 3, 10; t) = -(1/70)(B_2/B_0)^2 B_2(a^3 \dot{b}/b^3 c)$

Response of Trapped Particles. This analytical representation of the \mathbf{E} field induced by a time-varying model \mathbf{B} field is especially useful for following the response of trapped particles to a magnetic impulse. Each particle experiences an electric drift at velocity

$$\mathbf{v}_d = (c/B^2) \mathbf{E} \times \mathbf{B} \quad (3.06)$$

in addition to its gradient, curvature, and other (*cf.* Section III.6) drifts. As a consequence, the particle may change its value of L ($\equiv 2\pi a^2 B_0 |\Phi|^{-1}$).

Except for particles mirroring at the equator, the bounce average required in applying (3.06) is quite onerous. A rather different approach, based on (1.77b), is more expedient for calculating the radial-diffusion coefficient D_{LL} to lowest order in (B_2/B_0) , for arbitrary mirror latitude.

The more expedient approach is based on the fact that \mathbf{v}_d , as given by (3.06), can be identified as the local velocity of a field line if the \mathbf{E} field induced by $\partial\mathbf{B}/\partial t$ is everywhere perpendicular to \mathbf{B} . In other words, if only the $\mathbf{E}\times\mathbf{B}$ drift is considered, the particle remains on its original field line, as identified by the label L_d . The proof that field-line motion can be traced in this manner follows from the identity

$$\begin{aligned} B^2(dL_d/dt) &= B^2(\partial L_d/\partial t) + B^2\mathbf{v}_d\cdot\nabla L_d \\ &= B^2(\partial L_d/\partial t)(db/dt) + c\mathbf{E}\times\mathbf{B}\cdot\nabla L_d = 0, \end{aligned} \quad (3.07)$$

which can be verified with the aid of Table 7 to each order in ε_1 and ε_2 (see Section I.7). The degree of accuracy inherent in (1.69b), which implies

$$\begin{aligned} L_d &\approx (r/a \sin^2 \theta) [1 + (B_1/2B_0)(r/b)^3 \\ &\quad - (2B_2/21B_0 \sin \theta)(r/b)^4 (7 \sin^2 \theta - 3) \cos \varphi], \end{aligned} \quad (3.08)$$

is adequate to verify (3.07) in first and second order²². A more extensive proof (to higher order) is not required here, but could easily be generated [32].

Whereas the $\mathbf{E}\times\mathbf{B}$ drift induced by a time variation of b yields no immediate change in a particle's L_d coordinate, the gradient-curvature drift does. According to (1.77b) this change is of the form

$$dL_d/dt \approx -\dot{\varphi}(B_2/252B_0)L_d^5(a/b)^4 [Q(y)/D(y)] \sin \varphi. \quad (3.09)$$

The coordinate L_d to which the particle would return at $\varphi = \pm\pi/2$ in a magnetosphere frozen in time ($db/dt=0$) properly labels the drift shell in the sense that

²²The field-line label L_d defined by (1.51b) is conceptually useful only if higher internal geomagnetic multipoles, which would dominate the dipole as r approaches zero, are neglected. More generally, a field line may be labeled by the point at which it is anchored in the surface of an ideally conducting solid (of which the earth is an adequate example on the time scales of interest). If due account is taken of currents thereby induced on the surface of this conducting solid, it can be shown that the $\mathbf{E}\times\mathbf{B}$ drift induced by $\partial\mathbf{B}/\partial t$ impels a particle to remain attached to its original field line, as identified by the coordinates of its foot on the conducting surface [32]. In a model such as (1.45) there is no provision for currents at $r=a$, and the conducting solid degenerates to a point at the origin ($r=0$).

$$\begin{aligned} |\Phi| &= \int_0^{2\pi} \int_{r_e(\varphi)}^{\infty} B_0(a/r)^3 r dr d\varphi \\ &\quad - \int_0^{2\pi} \int_0^{r_e(\varphi)} [B_1(a/b)^3 - B_2(a/b)^3(r/b) \cos \varphi] r dr d\varphi \\ &= [2\pi a^2 B_0/L_d(\pi/2)] \{1 + O(\varepsilon_2^2) + \dots\}. \end{aligned} \quad (3.10)$$

For convenience, the third invariant has been evaluated using the equatorial plane ($\theta = \pi/2$) of the magnetosphere, in which case \mathbf{B} points in the $-\hat{\theta}(\pm\hat{z})$ direction and has a magnitude given by (1.45b). Since the end result of (3.10) has no correction terms of order ε_1 or ε_2 , the definition $L \equiv L_d(\pm\pi/2)$ suffices for a calculation of D_{LL} to lowest order.

Diffusion Coefficient. Since $L \equiv L_d(\pm\pi/2)$, it follows from (1.77b) that

$$L = L_d \{1 - (B_2/252B_0)(L_d a/b)^4 [Q(y)/D(y)] \cos \varphi\}. \quad (3.11)$$

The instantaneous shell parameter L thus changes at a rate

$$dL/dt = (B_2/63aB_0)(L a/b)^5 (db/dt) [Q(y)/D(y)] \cos \varphi \quad (3.12)$$

to lowest order in ε_1 and ε_2 . The radial diffusion coefficient $D_{LL} \equiv (1/2\tau) \langle (\Delta L)^2 \rangle$ is obtained by integrating (3.12) over an interaction time $\tau \gg 2\pi/\Omega_3$, during which $\cos \varphi = \cos(\Omega_3 t + \varphi_3)$. It is convenient to express the result in terms of $\mathcal{B}_z(\omega/2\pi)$, which is defined as the spectral density function of $B_1(a/b)^3$. The procedure for obtaining D_{LL} is much the same as that used in Section II.4, and the result [56, 57] is

$$D_{LL} = 2\Omega_3^2 (B_2/756B_1B_0)^2 L^5 (a/b)^2 [Q(y)/D(y)]^2 \mathcal{B}_z(\Omega_3/2\pi). \quad (3.13)$$

When radial diffusion is caused by magnetic impulses, the energy dependence of D_{LL} is contained entirely in Ω_3 . If the impulses rise sharply and decay slowly (like a step function) on the drift time scale, then $\mathcal{B}_z(\Omega_3/2\pi)$ is proportional to Ω_3^{-2} and *all energy dependence disappears*. At sufficiently high energies, the particle drift period becomes somewhat comparable to the rise time of an impulse (see Fig. 22), and this range of drift frequencies finds $\mathcal{B}_z(\Omega_3/2\pi)$ falling more sharply than Ω_3^{-2} . It follows that D_{LL} ultimately decreases somewhat with increasing energy. At constant M and J , however, the drift frequency decreases with increasing L . Thus, any inverse dependence of D_{LL} on particle energy tends to strengthen the L dependence of the radial-diffusion coefficient.

The dependence of D_{LL} on equatorial pitch angle is contained primarily in the factor $[Q(y)/D(y)]^2$. This factor, as approximated within $\sim 1\%$ by means of (1.36) and (1.79), varies by nearly an order of magnitude

between $y=1$ and $y=0$ [56, 57]. The function $Q(y)/180D(y)$ is plotted in Fig. 25. At energies sufficiently high that the drift period is comparable to the rise time of a magnetic impulse, this extreme variation of D_{LL} with x is slightly moderated by the fact that particles having $x \sim 1$ drift more slowly in azimuth than those for which $x=0$ [see (1.35)]. At a given energy, of course, this variation of Ω_3 with x is very weak.

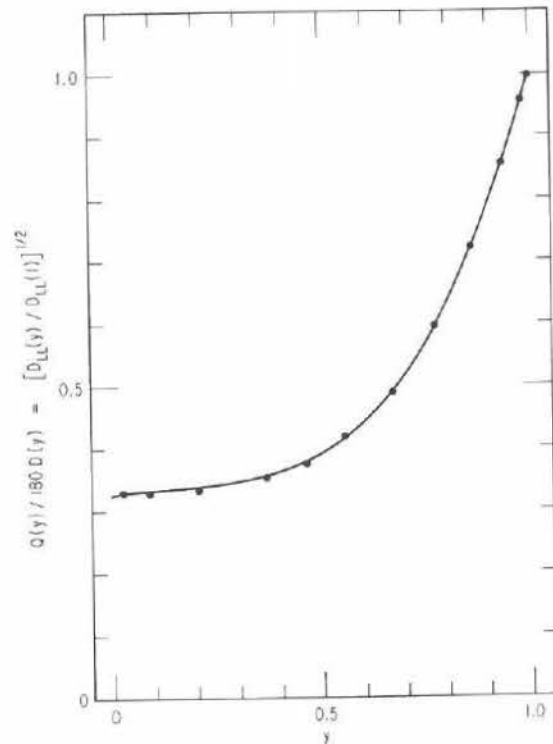


Fig. 25. Variation of $(D_{LL})^{1/2}$ with y for radial diffusion caused by magnetic sudden impulses. Data points have been determined by numerical computation [19]. Solid curve is analytical approximation [66] based on (1.36) and (1.79).

In summary, the radial-diffusion coefficient caused by magnetic impulses that rise sharply and decay slowly on the drift time scale is virtually independent of energy. For particles mirroring at the equator, the coefficient is given [29] by

$$D_{LL} = 2\Omega_3^2 (5B_2/21B_1B_0)^2 L^{10} (a/b)^2 \mathcal{B}_z(\Omega_3/2\pi) \quad (3.14)$$

since $Q(1)=180D(1)$. In the case that $\mathcal{B}_z(\Omega_3/2\pi)$ falls off as Ω_3^{-2} , there is no energy dependence in D_{LL} . Thus, the diffusion coefficient depends on y through the factor $[Q(y)/D(y)]^2$ in (3.13), and on L through the factor L^{10} . But since y and L are related via (3.02), the factor $[Q(y)/D(y)]^2$ exhibits an inverse variation with L . Except at $y=0$ and $y=1$, this factor tends to moderate the variation of D_{LL} with L . With the aid of Fig. 25, it is possible to evaluate the ratio of D_{LL} at any L to D_{LL} at $L=7$ and $y=1$ for selected values of y_7 , under the assumption that $\omega^2 \mathcal{B}_z(\omega/2\pi)$ is a constant. The results, plotted in Fig. 26, are principally of interest for high-energy protons and helium ions, which may in fact escape pitch-angle diffusion during their period of residence in the magnetosphere.

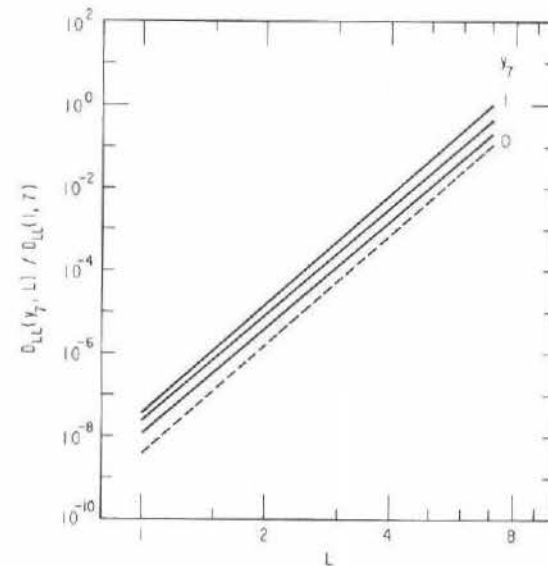


Fig. 26. Radial variation of D_{LL} driven by magnetic impulses, for selected values of y at $L=7$ ($y_7=0, 0.4, 0.6, 1.0$). Dashed line ($y_7=0$) is not realized in practice, because of the loss cone.

The magnitude of the spectral density function $\mathcal{B}_z(\omega/2\pi)$ is likely to vary with magnetic activity (as measured by an index such as K_p or D_{st}), and so the otherwise arbitrary interaction time τ used in this chapter is limited by the time scale of several days characteristic of changes in magnetospheric "weather". However, if the observations of \bar{f} are sufficiently coarse-grained as to average over genuine temporal variations of D_{LL} , it may be possible to identify a mean diffusion coefficient applicable to a much longer time interval (see Chapter V). Particle

lifetimes in the inner proton belt are even long enough (see Fig. 14, Section II.2) to permit averaging D_{LL} and \bar{f} over a large number of solar cycles.

III.3 Electrostatic Impulses

Abrupt temporal changes in the electrostatic potential associated with plasma convection are characteristic of geomagnetic storms and magnetospheric substorms. Impulses of this type can be represented by a time-dependent coefficient E_c in (1.52). For particles of radiation-belt energy ($W \gg |qV_c|$), the drift-shell asymmetry caused by the *mean* value of E_c can be neglected in the calculation of D_{LL} to lowest order in $qE_c a L_d / W$. Moreover, the magnetic field is assumed to be given by (1.16). In this situation it is evident from (1.66) that $|\Phi| = 2\pi a^2 B_0 / L_d(0)$, with no first-order correction in $qE_c a L_d / W$. Thus, the instantaneous shell parameter L is given in lowest order by

$$\begin{aligned} L &= L_d \{ 1 - [\gamma/(\gamma^2 - 1)] (qE_c a L_d / 3m_0 c^2) [T(y)/D(y)] \sin \varphi \} \\ &= L_d \{ 1 - (E_c/B_0)(c/\Omega_3 a) L_d^2 \sin \varphi \}, \end{aligned} \quad (3.15)$$

in view of (1.35). Since (1.65a), to the order of accuracy inherent in (3.15), implies that

$$dL_d/dt = \dot{\varphi} (E_c/B_0)(c/\Omega_3 a) L_d^2 \cos \varphi \quad (3.16)$$

for a particle drifting in azimuth under the influence of (1.52), it follows that

$$dL/dt = -(\dot{E}_c/B_0)(c/\Omega_3 a) L_d^3 \sin \varphi \quad (3.17)$$

for this particle. With E_c represented as the sum of purely temporal Fourier components [cf. (2.28)], the particle selects that component for which $\omega = \Omega_3$ after an interaction time $\tau \gg 2\pi/\Omega_3$.

The diffusion coefficient $D_{LL} \equiv (1/2\tau) \langle (\Delta L)^2 \rangle$ obtained from (3.17) by the methods of Section II.4 is given by

$$D_{LL} = 2(c/4aB_0)^2 L^6 \mathcal{E}_c(\Omega_3/2\pi), \quad (3.18)$$

where $\mathcal{E}_c(\omega/2\pi)$ is the spectral density function of E_c (see Section I.6). A particle's energy and equatorial pitch angle enter (3.18) only via Ω_3 . For electrostatic impulses that rise sharply and decay slowly on the drift time scale, the spectral density $\mathcal{E}_c(\Omega_3/2\pi)$ falls as Ω_3^{-2} . In this case, the functional form of D_{LL} is

$$\begin{aligned} D_{LL} &= 2(qa/24B_0)^2 L^{10} [T(y)/D(y)]^2 (y^2/M)^2 \\ &\quad \times [1 + (2MB_0/m_0 c^2 y^2 L^3)] \omega^2 \mathcal{E}_c(\omega/2\pi), \end{aligned} \quad (3.19)$$

where $\omega/2\pi$ is any frequency whose reciprocal lies well between the rise and decay times of the typical electrostatic impulse.

It is conventional to compare spatially coincident magnetospheric fluxes of different ionic species at common kinetic energy per nucleon, *i.e.*, at common particle velocity. This convention greatly simplifies the comparative analysis of collisional effects (see Section II.2). The ions of interest are typically nonrelativistic, and so the comparison applies essentially at common y , L , and M/A , where A is the number of nucleons in the ion. The respective electrostatic radial-diffusion coefficients thus scale as $(q/A)^2$. The magnitudes of D_{LL} for $H^+ : He^{++} : He^+$ therefore scale as 16:4:1. When coupled with the expectation that magnetospheric helium nuclei (originally interplanetary alpha particles) spend up to half their radiation-belt lifetimes as He^+ by virtue of charge exchange (see Section II.2), this property of electrostatic diffusion provides a possibly interesting explanation [40] for the observational fact (see Section IV.5) that ratios of helium-ion flux to proton flux (often abbreviated α/p and He^+/p) at common E/A in the magnetosphere (well off the equator) are orders of magnitude smaller than the α/p ratio in the solar wind [59].

Among particles of the same species, the diffusion coefficient given by (3.19) is rather sensitive to particle energy, but notably insensitive

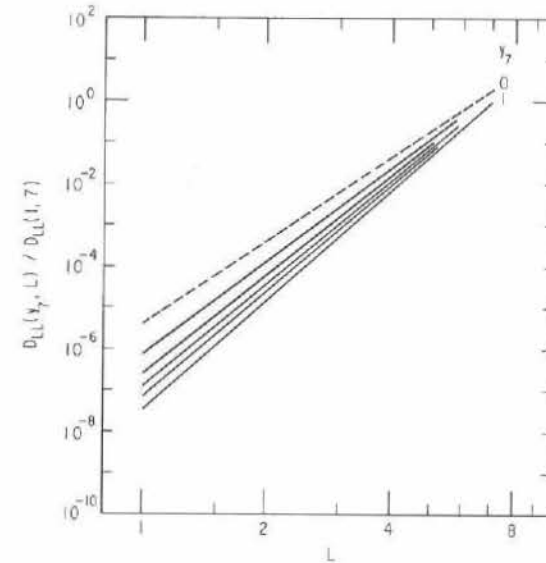


Fig. 27. Radial variation of D_{LL} driven by electrostatic impulses, for nonrelativistic particles having a common value of E at $L=7$ and selected values of y at $L=7$ ($y_7=0, 0.2, 0.4, 0.6, 0.8, 1.0$). Dashed line ($y_7=0$) is not realized in practice.

to equatorial pitch angle. Neither energy nor pitch angle is invariant during radial diffusion at constant M and J , however. Thus, a proper comparison should follow the spirit of Fig. 26, wherein particles are distinguished according to their values of y at $L=7$ in a dipole field. In electrostatic diffusion it is logical to compare particles having a common kinetic energy E_7 at $L=7$, i.e., a common value of M/y_7^2 . The derivation of (3.19) assumes that $\omega^2 \mathcal{E}_c(\omega/2\pi)$ is constant for all frequencies of interest. If attention is limited to nonrelativistic particles, such as radiation-belt ions, the variation of D_{LL} with L is that of $L^{10} [T(y)/D(y)]^2 (y/y_7)^4$. With the aid of Fig. 24, which indicates the variation of y with L for selected values of y_7 , the ratio of D_{LL} at arbitrary L to D_{LL} at $L=7$ and $y=1$ has been evaluated for these selected values of y_7 . The result is shown in Fig. 27. The common value of E_7 that forms the basis of this comparison is assumed to be such that $270 E_7 \ll m_0 c^2$ in order to justify using the nonrelativistic form of (3.19) down to $L \approx 1.08$, where the dense atmosphere terminates the inner belt (see Section II.2).

Spectral Density. Extrapolation of (3.19) to ring-current energies and below is forbidden on a variety of grounds. Consider (for example) a random sequence of impulses, each consisting of an ideally instantaneous jump from E_c to $E_c + \Delta E_c$, followed by an exponential decay to E_c with an e -folding time τ_d . The spectral density $\mathcal{E}_c(\omega/2\pi)$ is then given²³ by

$$\mathcal{E}_c(\omega/2\pi) = \frac{2(\tau_d^2/\tau) \Sigma(\Delta E_c)^2}{1 + \omega^2 \tau_d^2}, \quad (3.20)$$

where $\omega > 0$ and $\Sigma(\Delta E_c)^2$ denotes the sum of the squares of all sudden increments in E_c initiated within an arbitrarily long (but statistically homogeneous) time interval of duration τ . The validity of (3.19) thus requires $\omega^2 \tau_d^2 \gg 1$ at $\omega = |\Omega_3|$. It is presumed that $\tau_d \sim 2$ hr, and that most radiation-belt particles therefore comply with the conditions of (3.19). At ring-current (hot-plasma) energies and below, it is essential to reconsider the radial-diffusion problem in terms of (1.65), without making the simplifying approximation that $W \gg |qV_e|$.

On the other hand, the spectral density $\mathcal{E}_c(\Omega_3/2\pi)$ falls more rapidly than Ω_3^{-2} for particles having drift periods comparable to or smaller than the rise time of a typical impulse. The approximation of a vanishing rise time, as used in (3.20), is appropriate only if the particles of interest

²³The spectral density function given by (3.20) has been constructed in a manner easily generalized to other types of impulses. For example, if E_c is replaced by $B_1(a/b)^3$ in (3.20), the result is a formula for $\mathcal{B}_2(\omega/2\pi)$, the spectral density function for magnetic sudden impulses (Section III.2).

have drift periods well in excess of the true rise time. Moreover, the magnitude of $\mathcal{E}_c(\omega/2\pi)$ is likely to vary with the level of geomagnetic activity, as measured by an index such as K_p or D_{st} (cf. Section III.2).

Harmonic Resonances. Large-scale electrostatic fields in the magnetosphere presumably may fluctuate in other than the simple mode assumed in (3.17). For example, it may be impossible to represent the fluctuating $V_e(r, \theta, \varphi; t)$ as in (1.52), but quite reasonable to represent it as

$$V_e(r, \theta, \varphi; t) = \sum_m E_m(L_d, t) a L_d \sin(m\varphi + \psi_m). \quad (3.21)$$

The case culminating in (3.18) is included in (3.21) if $E_1(L_d, t) = E_c(t)$ and $\psi_1 = 0$. The more general expression for $V_e(r, \theta, \varphi; t)$, however, yields a diffusion coefficient of the form [56]

$$D_{LL} = 2(c/4aB_0)^2 L^9 \sum_m m^2 \mathcal{E}_m(L, m\Omega_3/2\pi), \quad (3.22)$$

where $\mathcal{E}_m(L, \omega/2\pi)$ is the spectral density function of $E_m(L_d, t)$. The additional spatial structure present in (3.21) thus partially transfers the burden of causing radial diffusion to the higher harmonics of the drift frequency. The entry of these higher harmonics is reminiscent of a similar effect in bounce-resonant pitch-angle diffusion (see Section II.4) and occurs for an analogous reason (lack of positive long-range spatial correlation). Magnetospheric observations of a fluctuating electrostatic field must therefore be treated with caution in terms of extracting a diffusion coefficient, unless the extent of spatial coherence is known.

III.4 Bounce Resonance

Resonance of an MHD or electrostatic wave with harmonics of a particle's bounce frequency has been invoked previously (see Section II.4) as a mechanism for pitch-angle diffusion. There it was noted that confinement of the electric-field perturbation \mathbf{e} to a meridional plane would prevent contamination by radial-diffusion effects. Conversely, a component of \mathbf{e} in the azimuthal direction provides for the possibility of radial diffusion. The case of an electrostatic wave (for which \mathbf{e} is parallel to \mathbf{k}) propagating purely in the azimuthal direction (see also Section III.5) is essentially covered by (3.21) and (3.22). The resonance condition is found to be $\omega = m\Omega_3$. Even if m is a very large number ($\sim \varepsilon^{-1}$ for a resonant particle), the resonance condition is unaffected by the bounce motion if \mathbf{k} is everywhere normal to \mathbf{B} for an electrostatic wave.

If, however, the electrostatic wave is such that field lines are *not* equipotentials, *e.g.*, as in (2.37), then the condition for resonance takes on the form [64]

$$\omega - m\Omega_3 - l\Omega_2 = 0. \quad (3.23)$$

Just as in (2.33), the various values of l enter the diffusion coefficient weighted by $J_l^2(k_{\parallel} p x / \gamma m_0 \Omega_2)$, which is small if the order (l) is much larger than the argument ($k_{\parallel} p x / \gamma m_0 \Omega_2$). If $m \ll |\epsilon|^{-1}$, it may be instructive to define an azimuthal wavenumber $k_{\phi} \equiv (m/r) \csc \theta$ and a bounce-averaged particle drift velocity $v_{\phi} = \Omega_3 r \sin \theta$ in the dipole field. The resonance condition then reads

$$\omega - k_{\phi} v_{\phi} = l\Omega_2, \quad (3.24)$$

which may be interpreted as a Doppler-shifted bounce resonance by analogy with (2.38). On the other hand, if $|m\Omega_3| \gg |l\Omega_2|$, it may be instructive to view (3.23) as a bounce-modified drift resonance. Since the two interpretations are fully equivalent for any m and l , however, the connection with radial diffusion (Section III.3) is quite evident.

A similar connection may be drawn between the magnetic impulses of Section III.2 and an MHD wave propagating partly in the direction of ∇L_d and partly in the directions of \mathbf{B} and $\hat{\phi}$. The electric-field perturbation \mathbf{e} for an MHD mode is normal to \mathbf{k} and \mathbf{B} (in the cold-plasma approximation), and thus lies in the plane of $\hat{\phi}$ and ∇L_d . The $\hat{\phi}$ component of \mathbf{e} leads to radial diffusion, the $\hat{\phi}$ component of \mathbf{k} to drift resonance, and the \mathbf{B} component of \mathbf{k} to bounce resonance. The condition imposed by (3.23) includes both bounce resonance and drift resonance. Either can be isolated by assigning $m=0$ or $l=0$, respectively.

III.5 Cyclotron Resonance

Because it leads to substantial pitch-angle diffusion, the Doppler-shifted ($k_{\parallel} v_{\parallel}$) cyclotron resonance considered in Section II.5 is principally a loss mechanism for geomagnetically trapped particles. Cyclotron resonance is not known to be an important mechanism for *radial* diffusion in the radiation belts. A particle is perhaps displaced by one gyroradius in the course of diffusing by one radian in pitch angle. In the absence of shell splitting (see Sections I.7 and III.7), the resulting radial-diffusion coefficient is of order $\epsilon^2 L^2 D_{xx}$. This is rather insignificant for radiation-belt ($|\epsilon| \ll 1$; Section I.1) particles, since the root-mean-square displacement in L is only of order ϵL during the lifetime of a particle (in weak diffusion; see Section II.7). The most energetic radiation-belt ions (for which $|\epsilon|$ is nearest to unity) tend to deposit their energy in the tenuous atmosphere without significant change of pitch angle.

The conditions under which radial diffusion might occur by virtue of cyclotron resonance are quite different from the conditions explored in Section II.5. Consider, for example, a wavelike electrostatic potential of the form

$$V_e(r, \theta, \varphi; t) = a E_m(L_d) \sin(m\varphi - \omega t + \psi_m) \quad (3.25)$$

where $\omega/2\pi$ is of the order of a particle's gyrofrequency. A wave of this type may be generated by virtue of an unstable spatial gradient of \bar{f} , *e.g.*, $\partial \bar{f} / \partial L_d < 0$, with the conserved quantities held constant. Such an azimuthally propagating wave is called a *drift wave*, whether or not cyclotron resonance is involved.

The unperturbed motion of an equatorially mirroring particle may be represented by

$$\varphi = \Omega_3 t + \varphi_3 + (pc/q B L_d a) \sin(\Omega_1 t + \varphi_1). \quad (3.26)$$

The postulated drift wave does not alter the equatorial pitch angle ($\pi/2$) of such a particle. The particle's interaction with the wave specified by (3.25) yields a φ_3 -dependent drift in L ($\equiv L_d$ in a dipole field) given by

$$\begin{aligned} dL/dt = & -(c/a)(L^3/B_0)m E_m(L) \sum_l J_l(-m v_{\perp}/\Omega_1 L a) \\ & \times \cos[(\omega - l\Omega_1 - m\Omega_3)t - (\psi_m + l\varphi_1 + m\varphi_3)]. \end{aligned} \quad (3.27)$$

The resonance condition $\omega = \omega_{lm} \equiv l\Omega_1 + m\Omega_3$ leads to a radial-diffusion coefficient of the form

$$D_{LL} = 2(c/2a B_0)^2 L^5 \sum_{lm} m^2 J_l^2(m v_{\perp}/\Omega_1 L a) \mathcal{E}_m(L, \omega_{lm}/2\pi), \quad (3.28)$$

where $\mathcal{E}_m(L, \omega/2\pi)$ is the spectral density of all waves having the form of (3.25). Note that m represents an *azimuthal index*, not a mass, in (3.25)–(3.28). The leading factors in (3.22) and (3.28) differ only because each term in (3.21) is a superposition of two waves having the form of (3.25).

In the argument of the Bessel function J_l , the factor m/La plays the role of k_{ϕ} in (3.24) or of k_{\perp} in (2.43). Thus, for azimuthal wavelengths comparable to a particle's gyroradius, a drift wave can resonate with the gyration of the particle in a manner that leads to radial diffusion. The pitch-angle of an equatorially mirroring particle is unaffected by this process, but the energy of a resonant particle changes in accordance with the relation

$$d(p^2)/dL = 2q \mathbf{p} \cdot \mathbf{e} (dL/dt)^{-1} = 2q \omega a^2 B_0 \gamma m_0 / mc L^2 \quad (3.29)$$

in a localized region where $dE_m/dL \approx 0$. The ratio m/q is negative for a wave (m) propagating in the direction of the resonant particle's azi-

muthal drift. Thus, an outward diffusive flow of trapped particles (arising from an inward gradient of \bar{f} with respect to L) leads to a transfer of particle energy to the wave²⁴. The interaction evidently conserves

$$p^2 - 2(q/m)(a^2 B_0 m_0/c) \int (\gamma \omega/L^2) dL = \text{constant}, \quad (3.30)$$

and so this is the quantity that must be held constant in evaluating $\partial \bar{f} / \partial L$. Although not known to play an essential role in radiation-belt dynamics, drift waves represent a potentially significant mechanism for extracting free energy from magnetospheric particle distributions by causing diffusion across field lines.

III.6 Bohm Diffusion

Electric Drift Velocity. In the absence of collisions and wave-particle interactions, the response of a charged particle to an electric field \mathbf{E}_\perp imposed across \mathbf{B} is the drift given by (1.53) or (3.06). For a simple derivation of this fact, consider that the transverse (to \mathbf{B}) electric field vanishes in a Lorentz frame moving at velocity \mathbf{v}_0 such that

$$c\mathbf{E}_\perp + \mathbf{v}_0 \times \mathbf{B} = \mathbf{0}. \quad (3.31)$$

If \mathbf{B} is uniform, a particle can only gyrate in this frame and execute translational motion along \mathbf{B} . The cross product between \mathbf{B} and (3.31) then yields (1.53) or (3.06) as the velocity of the Lorentz transformation, *i.e.*, of the guiding-center motion across \mathbf{B} . If \mathbf{B} is not uniform, then there are additional guiding-center forces equivalent to $q\mathbf{E}$. Replacement of $q\mathbf{E}$ in (1.53) or (3.06) by the sum of all forces \mathbf{F} acting on a particle yields a drift velocity

$$\mathbf{v}_d = (c/qB^2)\mathbf{F} \times \mathbf{B}. \quad (3.32)$$

The validity of (1.53) or (3.06) requires only that $v < c$. Guiding center forces requiring an average over gyration, *e.g.*, the forces $-(M/\gamma)\nabla B$ and $-(p_\perp^2/m)(\partial \mathbf{B}/\partial s)$ leading to gradient and curvature drifts (see Section I.5), limit (3.32) to drift velocities much less than $\epsilon \Omega_1 L a$ in absolute value. Since the gradient-curvature drift velocity is in fact of order $\epsilon^2 \Omega_1 L a$, this means only that the general validity of (3.12) is limited to $|\epsilon| \ll 1$, as previously assumed.

Effective Collision Frequency. In causing diffusion with respect to energy, pitch-angle, and L value, wave-particle interactions have an effect quite analogous to that of interparticle collisions. For this reason it is often

²⁴Drift waves can be destabilized under a variety of conditions [60]. The present calculation illustrates only one example.

convenient to think in terms of a effective collision frequency $1/\tau_\perp$ to which the various diffusion coefficients can be related, just as if interparticle collisions were the agent responsible for the diffusion. This equivalent collision frequency is said to produce anomalous transport, in the sense that the diffusion exceeds that which would result from Coulomb collisions acting alone. Thus, the quantity $1/\tau_\perp$ generally exceeds the Coulomb collision frequency.

The mean (phase-averaged) force exerted by collisions and wave-particle interactions can be represented by $-(m/\tau_\perp)\mathbf{v}_d$. If \mathbf{B} is uniform, therefore, the net drift velocity resulting from the imposition of \mathbf{E}_\perp across \mathbf{B} is given by

$$\begin{aligned} \mathbf{v}_d &= (c/B)\mathbf{E}_\perp \times \hat{\mathbf{B}} + (1/\Omega_1 \tau_\perp)\mathbf{v}_d \times \hat{\mathbf{B}} \\ &= \frac{(cE_\perp/B)(\Omega_1 \tau_\perp)}{1 + (\Omega_1 \tau_\perp)^2} [\Omega_1 \tau_\perp (\hat{\mathbf{E}}_\perp \times \hat{\mathbf{B}}) - \hat{\mathbf{E}}_\perp], \end{aligned} \quad (3.33)$$

where $\Omega_1 = -qB/mc$. This result indicates a *Hall mobility*

$$\mu_H = (c/B)(\Omega_1 \tau_\perp)^2 [1 + (\Omega_1 \tau_\perp)^2]^{-1} \quad (3.34a)$$

in the direction of $\hat{\mathbf{E}}_\perp \times \hat{\mathbf{B}}$ and a *Pedersen mobility*

$$\mu_\perp = -(c/B)(\Omega_1 \tau_\perp) [1 + (\Omega_1 \tau_\perp)^2]^{-1} \quad (3.34b)$$

in the direction of $\hat{\mathbf{E}}_\perp$. The Pedersen mobility approaches zero in the limit of no "collisions" ($\Omega_1^2 \tau_\perp^2 \gg 1$) and approaches $q\tau_\perp/m$ in the limit of "collision" dominance ($\Omega_1^2 \tau_\perp^2 \ll 1$). The maximum absolute value ($c/2B$) of μ_\perp is attained when $\Omega_1^2 \tau_\perp^2 = 1$.

Diffusion Coefficient. The purpose of calculating the Pedersen mobility is ultimately to obtain the diffusion coefficient related to it, *i.e.*, the coefficient for the stochastic transport of particles *across* adiabatic drift shells. The connection between mobility and diffusion is given [61] by $D_\perp = (p_\perp^2/2qm)\mu_\perp$. Since L is a dimensionless variable scaled by the earth radius a , the quantity D_\perp must be interpreted as $a^2 D_{LL}$. It follows that

$$D_{LL} = (p_\perp/ma)^2 (\tau_\perp/2) [1 + (\Omega_1 \tau_\perp)^2]^{-1}. \quad (3.35)$$

If τ_\perp is now considered an adjustable parameter, the magnitude of D_{LL} can be maximized by setting $\tau_\perp = |\Omega_1|^{-1}$. In other words, there exists an upper bound, given by

$$D_{LL}^* = (p_\perp/2ma\Omega_1)^2 |\Omega_1|, \quad (3.36)$$

on the coefficient of radial diffusion. No adjustment of τ_\perp can produce a value of D_{LL} larger than D_{LL}^* . A process in which $D_{LL} \sim D_{LL}^*$ is characterized as *Bohm diffusion* [62]. It represents the most expedient means

available to a hot plasma for erasing an unstable spatial gradient (cf. Section III.5) in the distribution function, and in this sense is analogous to strong pitch-angle diffusion (Section II.7), which has the same property relative to unstable gradients of \tilde{f} in momentum space.

There is, however, no reason why Bohm diffusion must cause strong pitch-angle diffusion. As in Section III.5, the "collisions" could easily act preferentially in the direction normal to \mathbf{B} , an option not available to interparticle collisions. Thus, the anomalous Ohmic mobility $\mu_{\parallel} \equiv (\mathbf{v} \cdot \hat{\mathbf{B}})/(\mathbf{E} \cdot \hat{\mathbf{B}})$ is given by $q\tau_{\parallel}/m$, where τ_{\parallel} may be entirely different in magnitude from τ_{\perp} in (3.34). In the event that $\tau_{\parallel} \gg \tau_{\perp}$, there may be very few particles scattered into the loss cone in the course of Bohm diffusion. Conversely, strong diffusion requires only that $\Omega_2 \tau_{\perp} \ll 1$ and $\Omega_2 \tau_{\parallel} \ll 1$. These conditions do not necessarily imply $|\Omega_1| \tau_{\perp} \sim 1$, as required for Bohm diffusion.

An examination of (3.36) indicates that $D_{LL}^* \sim L^2 |\Omega_3|$. No radiation-belt observations are known to require nearly this large a value of D_{LL} , but the storm-time ring current occasionally appears to exhibit Bohm diffusion in the vicinity of the plasmapause. The plasmasphere tends to destabilize the ring current against electromagnetic ion-cyclotron turbulence (see Section II.6) by drastically reducing the minimum resonant energy given by (2.69b). Bohm diffusion is sometimes invoked [63], in addition to the adiabatic gradient-curvature drift, as a means of transporting ring-current protons into the plasmasphere from the exterior region in which N_p is very small ($\sim 0.1 \text{ cm}^{-3}$ during a magnetic storm). Even in the presence of strong pitch-angle diffusion, which the resulting ion-cyclotron turbulence causes, the Bohm diffusion coefficient would transport ring-current protons ($\epsilon \sim 10^{-3}$) a root-mean-square distance $\sim 0.5a$ relative to the plasmapause during the lifetime $1/\lambda$ given by (2.77).

III.7 Shell Splitting

As described in Section I.7, drift-shell splitting is a purely adiabatic phenomenon that violates none of the invariants. Radial diffusion, by definition, violates the third invariant. Pitch-angle diffusion violates either or both of the first two invariants, usually both. In a symmetrical magnetosphere, the incidentally associated radial diffusion coefficient $D_{LL} (\sim \epsilon^2 L^2 D_{xx})$ would be too small to be of significance for radiation-belt particles ($\epsilon^2 \ll 1$). In the presence of azimuthal asymmetry and shell splitting, however, pitch-angle diffusion *automatically* produces an additional violation of the third invariant. The shell-tracing results obtained

in Section I.7 permit this effect to be evaluated for arbitrary values of the equatorial pitch angle.

The basic equation governing the process under consideration is (cf. Section II.2)

$$D_{LL} = \langle (\partial L / \partial x)^2 D_{xx} \rangle = \langle (x/y)^2 (\partial L / \partial y)^2 D_{xx} \rangle. \quad (3.37)$$

Thus, if the values of $L (\equiv 2\pi a^2 B_0 |\Phi|^{-1})$, among identical particles having mirror points on a common field line, vary with equatorial pitch angle, then pitch-angle diffusion of these particles on this field line automatically produces diffusion with respect to L [5]. The partial derivatives are evaluated by holding constant the quantity conserved by D_{xx} , typically the particle energy or first invariant. The drift average denoted by the angle brackets necessarily yields a positive-definite D_{LL} [65].

External Multipoles. In the case of magnetic shell splitting, as summarized by (3.11), pitch-angle diffusion leaves L_a and φ invariant at the scattering site, and so the quantity $\partial L / \partial y$ is given by

$$\begin{aligned} \partial L / \partial y = & -(B_2 / 252 B_0) (a/b)^4 L_a^5 [D(y)]^{-2} \\ & \times [Q'(y)D(y) - D'(y)Q(y)]. \end{aligned} \quad (3.38)$$

If pitch-angle diffusion is distributed uniformly with respect to longitude, *i. e.*, if D_{xx} is independent of φ , then to lowest order in $\epsilon_2 \equiv (B_2/B_0)(L_a a/b)^4$ it follows that

$$\begin{aligned} D_{LL} = & (x^2/2y^2)(B_2/252B_0)^2 (a/b)^8 L^{10} [D(y)]^{-4} \\ & \times [Q'(y)D(y) - D'(y)Q(y)]^2 D_{xx}. \end{aligned} \quad (3.39)$$

With the aid of (1.36) and (1.79), the function $(x^2/98y^2)[6D(y)]^{-4} \times [Q'(y)D(y) - D'(y)Q(y)]^2$, which expresses the pitch-angle dependence of D_{LL}/D_{xx} , has been plotted in Fig. 28 [66]. This function reduces to $25x^2/18$ in the limit $x^2 \equiv 1 - y^2 \ll 1$, in which case (3.39) reduces to the expression

$$\begin{aligned} D_{LL} \approx & (x^2/18)(5B_2/B_0)^2 (a/b)^8 L^{10} D_{xx} \\ \approx & 0.61 x^2 (a/b)^8 L^{10} D_{xx}. \end{aligned} \quad (3.40)$$

As an upper bound on radial diffusion induced by magnetic shell splitting, this expression remains valid for $|x| \leq 0.9997$; it fails only deep within the loss cone. As an approximate expression for D_{LL} , equation (3.40) remains valid within a factor of two only for $|x| \leq 0.6$, while (3.39) is correct to within a few percent for all x when evaluated via (1.36) and (1.79).

The complete Jacobian entering (2.12), when pitch-angle diffusion violates Φ , depends upon the nature of the quantity conserved in the

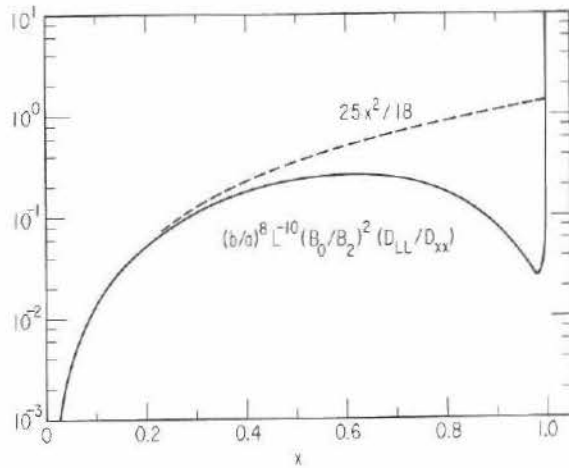


Fig. 28. Relation between D_{LL} and D_{xx} for shell splitting caused by noon-midnight magnetic asymmetry [66], as given by harmonic-bounce approximation (dashed curve) and by improved approximation (solid curve) based on (1.36) and (1.79).

process. If the conserved quantity is particle energy, then the relevant Jacobian is

$$G(M, J, |\Phi|; E, x, L) = -8\pi\gamma p L^2 a^3 x T(y), \quad (3.41a)$$

as deduced from (2.14) and (1.37). If, as in the case of bounce resonance, the conserved quantity is M , then the relevant Jacobian is

$$G(M, J, |\Phi|; M, x, L) = -8\pi B_0 a^3 (p/y^2 L) x T(y), \quad (3.41b)$$

which follows from (2.27), (1.37), and the fact that $(\partial w/\partial x)_{M,L} = 2MB_0 x/L^3 y^4$ [cf. (2.33) and (2.34)].

In (3.41a), the distribution function \bar{f} is considered to depend on E , x , and L . Since E is conserved by the process, the distribution function satisfies [65]

$$\frac{\partial \bar{f}}{\partial t} = \frac{1}{L^2} \frac{\partial}{\partial L} \left[L^2 D_{LL} \frac{\partial \bar{f}}{\partial L} \right]_x + \frac{1}{x T(y)} \frac{\partial}{\partial x} \left[x T(y) D_{xx} \frac{\partial \bar{f}}{\partial x} \right]_L, \quad (3.42)$$

where D_{LL} is given by (3.39). This equation contrasts strikingly with (3.01), which applies to processes that conserve M and J .

Electric Shell Splitting. In the case of electric shell splitting, caused by superposition of (1.52) upon the dipole field (1.16), the relation between L and y at constant L_d and φ is expressed by (3.15), provided that

$W \gg |qV_e|$ around the entire drift shell. The connection between D_{LL} and a φ -independent D_{xx} is then given by

$$D_{LL} \approx (qE_c a L^2/W)(m_0 c^2 + W)^2 (2m_0 c^2 + W)^{-2} [6D(y)]^{-4} \times [Y'(y)T(y) - T'(y)Y(y)]^2 (x^2/2y^2) D_{xx} \quad (3.43)$$

for pitch-angle diffusion at constant particle energy W . With the aid of (1.28), (1.31), and (1.36), the function $(x^2/8y^2)[6D(y)]^{-4}[Y'(y)T(y) - T'(y)Y(y)]^2$ has been plotted in Fig. 29. This function indicates the pitch-angle dependence of D_{LL}/D_{xx} in the presence of electric shell splitting, and approaches $x^2/162$ in the limit $x^2 \ll 1$. The nonrelativistic limit ($W \ll m_0 c^2$) of (3.43) therefore reads

$$D_{LL} \approx (x^2/162)(qE_c a L^2/W)^2 D_{xx} \quad (3.44)$$

for $x^2 \ll 1$, and represents a serious (factor-of-two) underestimate for D_{LL} only if $|x| \gtrsim 0.6$.

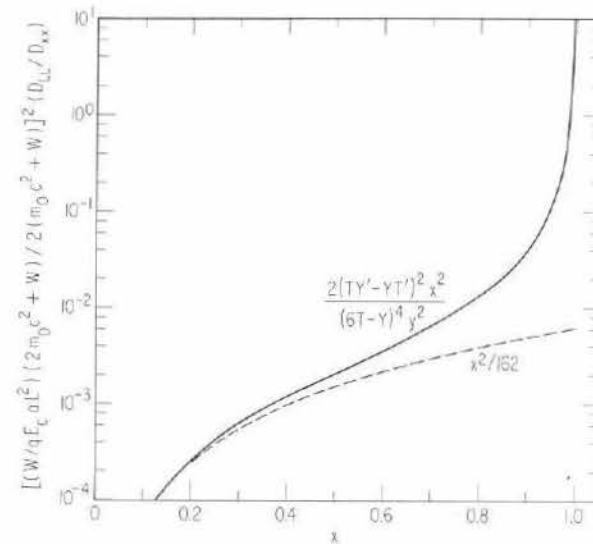


Fig. 29. Relation between D_{LL} and D_{xx} for shell splitting caused by dawn-dusk asymmetry of electrostatic potential [66], as given by harmonic-bounce approximation (dashed curve) and by improved approximation (solid curve) based on (1.28), (1.31), and (1.36).

A comparison between (3.40) and (3.44), assuming $b=10a$ and $E_c a=4$ kV, suggests that magnetic and electric shell-splitting effects are comparable at $M/y^2 \sim 7$ MeV/gauss, *i.e.*, at first invariants typical of

the ring-current particles. In the true radiation belts, magnetic shell splitting effects exceed those of electric shell splitting²⁵.

At particle energies below those typical of the ring current, it is necessary to reconsider the shell-splitting problem in terms of (1.65). Beyond the plasmapause, such drift shells do not close within the magnetosphere, and the corresponding third invariants are undefined (cf. Fig. 12, Section I.6). Within the plasmasphere, all shell splitting disappears in the cold-plasma limit, since "zero-energy" particles drift on field-aligned surfaces of constant electrostatic potential.

Internal Multipoles. At very low L values, certain internal geomagnetic multipoles associated with true field anomalies, may cause significant shell splitting among inner-belt particles [67]. If electric fields are negligible, the existence of magnetic shell splitting in general can be demonstrated (cf. Section I.7) by showing that $(\partial^2 B / \partial s^2)_e$ varies with φ around a path of constant B_e on the equatorial ($\partial B / \partial s = 0$) surface. This criterion follows from (1.26) and (1.32a), in the sense that the drift shell (which conserves M and J) must depart from the constant- B_e trajectory for $x \neq 0$ if Ω_2 varies with φ ; to lowest order in x , the bounce frequency is given by $\Omega_2^2 = (M/\gamma m)(\partial^2 B / \partial s^2)_e$.

In a dipole field, the value of $(\partial^2 B / \partial s^2)_e$ is given by $9B_0/a^2 L_m^5$, where $L_m^3 \equiv (B_0/B_e)$ at $y=1$ [cf. (1.38)]. It proves convenient to display the azimuthal variation of $(\partial^2 B / \partial s^2)_e$ at constant B_e and L_m by plotting $L_m^2 [(L_m^5 a^2 / 9B_0)(\partial^2 B / \partial s^2)_e - 1]$ against geomagnetic longitude. This is done²⁶ in Fig. 30 for $L_m = 1, 2$, and 7. The sinusoidal asymptote, approximated by the curve $L_m = \infty$, results from an internal octupole. The octupole corresponds to $n = -5$ in (1.46) and the dipole to $n = -3$, hence the factor L_m^2 in Fig. 30. Higher multipoles produce the broad South African anomaly (longitude $30^\circ - 120^\circ$) and the narrow South American anomaly (longitude $0^\circ - 30^\circ$). The latter disappears between $L_m = 1$ and $L_m = 2$. The fact that the dipole is off center by $\sim 0.07a$, toward longitude 217° , necessarily contributes nothing to shell splitting as this is not a field asymmetry. Components of the geomagnetic quadrupole that survive the transformation to offset-dipole coordinates can only warp the equatorial ($\partial B / \partial s = 0$) surface as a lowest-order effect. Their second-order (shell-splitting) effects are not discernible in Fig. 30 [67].

²⁵However, the demarcation between ring-current and radiation-belt parameters is somewhat arbitrary (Fig. 13, Section I.7).

²⁶The shell $L_m = 1$ is unphysical in the sense that it intersects the earth's surface (see Section II.7).

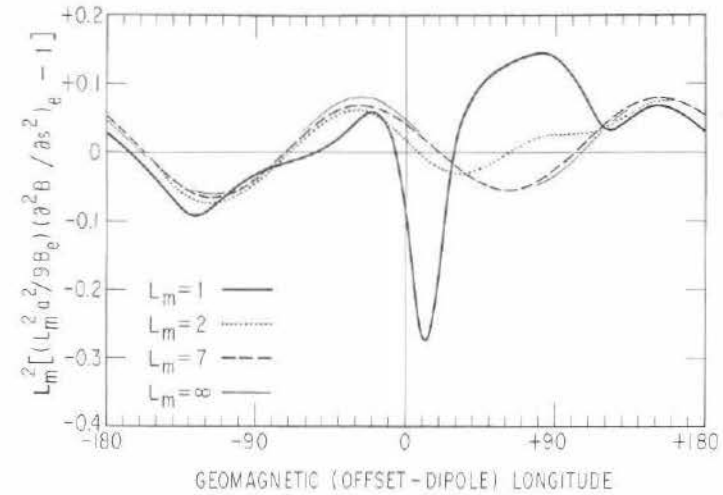


Fig. 30. Normalized shell-splitting function associated with internal geomagnetic multipoles, shown for selected contours of constant B on the equatorial surface [67].

True field anomalies (including the octupole) that significantly split drift shells thereby subject the inner radiation belt to radial diffusion coincident with pitch-angle scattering. A lower bound on the resulting D_{LL} is provided by the inequality

$$D_{LL} \geq (L_m x/3)^2 (L_m^5 a^2 / 9 B_0)^2 \times \text{Min} \langle [(\partial^2 B / \partial s^2)_0 - (\partial^2 B / \partial s^2)_e]^2 D_{xx} \rangle \quad (3.45)$$

where the angle brackets denote an equatorial drift average, which must be minimized with respect to some reference longitude φ_0 at which $(\partial^2 B / \partial s^2)_e \equiv (\partial^2 B / \partial s^2)_0$. The minimizing operation (Min) assures that (3.45) is a lower bound on the radial diffusion coefficient, regardless of the reference longitude that ultimately proves suitable for defining L [cf. (3.10)]. If the pitch-angle scattering is principally atmospheric (e.g., at $L_m \lesssim 1.25$ for inner-belt electrons), then the magnitude of D_{xx} is strongly φ -dependent, with a peak near geomagnetic longitude 20° (cf. Section II.2).

III.8 Diffusion in More Than One Mode

For each diffusion mechanism considered in Chapters II and III, the diffusion tensor D_{ij} (see Section II.1) can be diagonalized by a proper choice of variables, i.e., by transforming from the coordinates (M, J, Φ)

to an equivalent set of functionally independent variables. Mixed partial derivatives in (2.12) are thus eliminated. Vanishing eigenvalues (diagonal elements, $i=j$) of the transformed diffusion tensor \tilde{D}_{ij} correspond to conservation laws of the diffusion mechanism [68]. For example, *pure* pitch-angle diffusion, *i.e.*, diffusion at constant particle energy, corresponds to $D_{EE}=0$ and (in the absence of shell splitting) $D_{LL}=0$. Pure third-invariant diffusion (Sections III.1—III.3) has the property that $D_{MM}=D_{JJ}=0$. A summary of various diffusion mechanisms, their conservation laws, and the Jacobians of their respective diagonalizing transformations is given in Table 8.

Table 8. Diffusion Variables and Associated Jacobians

Interaction	Invariants	Relevant Jacobian
Elastic Collisions (without recoil)	$E, (\Phi)$	$ G(M, J, \Phi; E, x, L) $ $= 8\pi\gamma p L^2 a^3 x T(y)$
Cyclotron Resonance	$(E), (\Phi)$	$ G(M, J, \Phi; E, x, L) $ $= 8\pi\gamma p L^2 a^3 x T(y)$
Bounce Resonance	$M, (\Phi)$	$ G(M, J, \Phi; M, x, L) $ $= 8\pi(a/y)^3 (2m_0 B_0^3 M/L^2)^{1/2} x T(y)$
Drift Resonance	M, K	$ G(M, J, \Phi; M, K, L) $ $= (8m_0 M)^{1/2} (2\pi B_0 a^2/L^2)$
Bimodal Diffusion	(ζ)	$ G(M, J, \Phi; \zeta, x, L) $ $= 8\pi a^3 (2m_0 B_0^3 \zeta/L^2)^{1/2} x T(y)$

(Parenthesized "invariant" quantities are either approximately or conditionally conserved).

No special difficulty of concept arises when two or more diffusion mechanisms act simultaneously. If the concurrent processes satisfy the same conservation laws, then a single transformation of variables will suffice to make the diffusion tensor diagonal. If not, *i.e.*, if the conservation laws for kinematical variables are not common to the various diffusion mechanisms acting concurrently, then the problem is said to involve more than one *mode* of diffusion. In this case, the diffusion equation is at least two-dimensional with respect to the kinematical variables. This property presents no special difficulty, since two-dimensional diffusion equations, *e.g.*, (3.42), have already appeared in the context of unimodal diffusion. In constructing a bimodal diffusion equation, however, it is essential to evaluate the partial derivatives in accordance with the conservation laws of the respective modes. For example, if radial diffusion at constant M and J (coefficient D_{LL}) is superimposed upon pitch-angle diffusion at constant E (coefficient D_{xx}) in the presence of magnetic shell splitting, the equation governing this bimodal process is

$$\frac{\partial \bar{f}}{\partial t} = L^2 \frac{\partial}{\partial L} \left[\frac{1}{L^2} D_{LL} \frac{\partial \bar{f}}{\partial L} \right]_{M,J} + \frac{1}{x T(y)} \frac{\partial}{\partial x} \left[x T(y) D_{xx} \frac{\partial \bar{f}}{\partial x} \right]_{E,L} \quad (3.46)$$

$$+ \frac{1}{L^2} \frac{\partial}{\partial L} \left[\frac{x^2 L^2 [Q'(y)D(y) - D'(y)Q(y)]^2 D_{xx}}{2(252 B_0/B_2)^2 (b/a)^8 [D(y)]^4 y^2} \frac{\partial \bar{f}}{\partial L} \right]_{E,x},$$

a result obtained by consolidating (3.01), (3.39), and (3.42).

The right-hand side of (3.46) has the form of minus the "divergence" of a diffusion current for each mode (*cf.* Sections II.1 and II.2). The radial (trans- L) component of the diffusion current has the form $-D_{LL}(\partial \bar{f}/\partial L)_{M,J}$ for the sudden-impulse mode and the form $-\langle (x/y)^2 (\partial L/\partial y)^2 D_{xx} \rangle (\partial \bar{f}/\partial L)_{E,x}$ for the shell-splitting mode [*cf.* (3.37), Section III.7]. For outer-belt electrons at $L \gtrsim 5$, it is interesting that $(\partial \bar{f}/\partial L)_{M,J}$ is typically positive, while $(\partial \bar{f}/\partial L)_{E,x}$ is typically negative (see Fig. 1 and Section IV.6). The diffusion current across L thus consists of an *inward* part conserving M and J , which tends to energize the diffusing particles, and an *outward* part conserving E . The net result is that, for particles diffusing "bimodally" from an external source into the outer belt, the gain in energy typically *exceeds* that predicted on the basis of constant M and J [69] (see Section III.1).

Even if shell-splitting effects are neglected, *e.g.*, by taking $B_2=0$, the diffusion equation (3.46) is two-dimensional in the sense that no overall conservation law relates x and L . Thus, an individual particle from the distribution $\bar{f}(E, x, L; t)$ may random-walk a complete cycle in x and L , as illustrated in Fig. 31. In the absence of shell splitting,

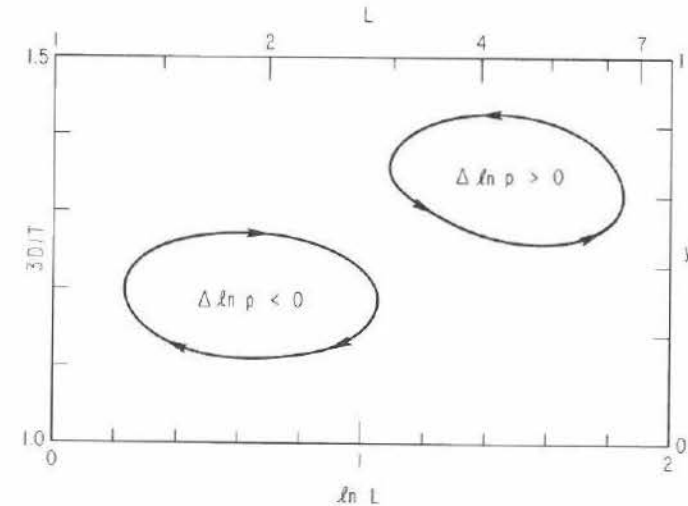


Fig. 31. Schematic illustration of particle cycles in bimodal diffusion.

the radial diffusion in (3.46) occurs at constant M and J . According to (1.34b), the variation of particle energy with L is governed by the relationship

$$(\partial \ln p / \partial \ln L)_{M,J} = -3 [D(y)/T(y)]. \quad (3.47)$$

It follows that a clockwise cycle in Fig. 31 (inward diffusion at generally smaller y than outward diffusion) represents a net loss in particle energy, while a counter-clockwise cycle causes a particle to gain energy. In this context, bimodal diffusion acts as a "thermalization" mechanism, whereby an initially narrow energy spectrum of particles can become distributed to both higher and lower energies than pure conservation of M and J would allow [69].

Reduced Diffusion Equations. For many problems involving radiation-belt diffusion, it is considered appropriate to simplify (3.46) by means of approximations that reduce the diffusion equation to one spatial dimension. Simplifying approximations of this type are often indicated when the observational data are not sufficiently complete to impose meaningful boundary conditions on (3.46). In many cases the observations cover too limited a range of parameter space to make full use of (3.46). Reduction of the diffusion equation to one dimension, however justified, does require that bimodal cycles of the type illustrated in Fig. 31 be neglected. This is part of the cost of analytical simplification.

A naive means of reducing (3.46) is to neglect shell-splitting effects and to replace the pitch-angle diffusion term by a simple loss term of the form $-\bar{f}/\tau$. In this approximation [70] the diffusion equation reads [cf. (2.09)]

$$\frac{\partial \bar{f}}{\partial t} = L^2 \frac{\partial}{\partial L} \left[\frac{1}{L^2} \bar{D}_{LL} \frac{\partial \bar{f}}{\partial L} \right] - \frac{\bar{f}}{\tau} \quad (3.48)$$

and applies to $\bar{f}(M, L; t)$ at $J=0$. The pitch angles of particles having in common their values of M/y^2 and L are mixed thoroughly on a time scale $\sim \tau/5$ (see Section II.7). The representation of pitch-angle diffusion as a simple loss term, as in (3.48), essentially requires that $5\bar{f}/\tau$ greatly exceed $\partial \bar{f} / \partial t$ in absolute value²⁷. The diffusion coefficient \bar{D}_{LL} is then interpreted as an average over particles sharing the same values of M/y^2 and L , respectively.

A more sophisticated view of the reduction described in the paragraph above is that a new variable $\zeta \equiv M/y^2$ has been introduced, and that ζ is *approximately* conserved by both D_{LL} and D_{xx} [71]. From this

²⁷This requirement is often overlooked in the interest of expedience.

viewpoint, the form of (3.48) should be governed by the Jacobian [5]

$$G(M, J, |\Phi|; \zeta, x, L) = -(8\pi a^3 B_0/L^{5/2}) x T(y) (2m_0 B_0 \zeta)^{1/2}, \quad (3.49)$$

which has been included in Table 8. With this Jacobian, the reduced (to one dimension) diffusion equation evidently has the form

$$\frac{\partial \bar{f}}{\partial t} = L^{5/2} \frac{\partial}{\partial L} \left[L^{-5/2} \bar{D}_{LL} \frac{\partial \bar{f}}{\partial L} \right] - \frac{\bar{f}}{\tau}. \quad (3.50)$$

The practical discrepancy between (3.48) and (3.50) is slight, amounting only to a square root of L in the metric. Since D_{LL} typically varies as L^{10} (see Sections III.2 and III.3) for radiation-belt particles, it is difficult to imagine that seriously different geophysical predictions might emerge from (3.48) and (3.50), although (3.50) is perhaps preferable in terms of self-consistency.

In either representation the transport coefficients may certainly vary with L , and perhaps also with ζ ($=M$ at $J=0$) and/or time. Since \bar{D}_{LL} and τ arise from operations on the entire pitch-angle distribution, it would be meaningless to give either a dependence on x or y . This degree of freedom has been sacrificed in reducing (3.46) to one dimension. The conservation of ζ is clearly an idealization that breaks down for $x \sim 1$, but the presence of a loss cone (see Section II.7) assures that \bar{f} is small there²⁸. Thus, the effective radial-diffusion coefficient \bar{D}_{LL} is heavily weighted by the behavior of particles for which $x^2 \ll 1$, *i.e.*, for which radial diffusion at constant M and J very nearly conserves ζ .

If the time scale for pitch-angle mixing ($\sim \tau/5$) is comparable to that for radial diffusion, then a simplified equation such as (3.50), which assigns to \bar{f} the lowest mode of pitch-angle diffusion (see Section II.7), cannot apply unless D_{LL} is substantially independent of x (cf. Sections III.2 and III.3). Thus, radial diffusion caused by electrostatic impulses may lend itself to analysis via (3.50), but that caused by magnetic impulses will ordinarily bias \bar{f} toward higher modes of pitch-angle diffusion. In this case a more general treatment is required.

If the need to circumvent (3.46) is compelling, it may be possible to expand $\bar{f}(\zeta, x, L; t)$ in pitch-angle eigenfunctions $g_n(x)$ that are even in x (even parity required because of homogeneity over bounce phase). An expansion [71] of the form

$$\bar{f}(\zeta, x, L; t) = \sum_n a_n(\zeta, L; t) g_n(x) \quad (3.51)$$

²⁸The constant- ζ approximation means that particles diffuse radially at constant y , in weak violation of (1.34a), (3.02), and Fig. 24.

with the boundary condition $g_n(x_c)=0$ is justified if x_c is independent of L , and the L dependence of D_{xx} is factorable, *i.e.*, if D_{xx} is the product of a function of L , ζ , and t times a function of x . These conditions on x_c and D_{xx} are probably well satisfied in the outer zone. It is convenient to assume further that D_{xx} and D_{LL} are time-independent. In this case the approximate diffusion equation [cf. (3.50), (3.49), and (3.46), with $B_2=0$ (*i.e.*, without shell splitting)]

$$\frac{\partial \bar{f}}{\partial t} = L^{5/2} \frac{\partial}{\partial L} \left[L^{-5/2} D_{LL} \frac{\partial \bar{f}}{\partial L} \right]_x + \frac{1}{x T(y)} \frac{\partial}{\partial x} \left[x T(y) D_{xx} \frac{\partial \bar{f}}{\partial x} \right]_L \quad (3.52a)$$

can be simplified by virtue of the eigenvalue property

$$\frac{1}{x T(y)} \frac{\partial}{\partial x} \left[x T(y) D_{xx} g_n(x) \right]_L = -\lambda_n(\zeta, L) g_n(x), \quad (3.52b)$$

where $\lambda_n(\zeta, L)$ is the decay rate characteristic of the pitch-angle eigenmode g_n (cf. Section II.7).

The normalized eigenfunctions corresponding to distinct eigenvalues λ_n are orthogonal in the sense that

$$\int_0^{x_c} x T(y) g_n(x) g_m(x) dx = \delta_{nm}. \quad (3.53)$$

Application of (3.52) to (3.51) therefore implies that

$$\frac{\partial a_m}{\partial t} = L^{5/2} \frac{\partial}{\partial L} \left[L^{-5/2} \sum_n \bar{D}_{LL}^{mn} \frac{\partial a_n}{\partial L} \right]_\zeta - \lambda_m a_m, \quad (3.54a)$$

where

$$\bar{D}_{LL}^{mn} \equiv \int_0^{x_c} x T(y) D_{LL} g_m(x) g_n(x) dx. \quad (3.54b)$$

If D_{LL} is independent of x , as is approximately true in radial diffusion caused by electrostatic impulses (see Section III.3), then the matrix \bar{D}_{LL}^{mn} is diagonal in the sense that $\bar{D}_{LL}^{mn} = D_{LL} \delta_{mn}$. In this case the functions $a_m(\zeta, L; t)$ and $a_n(\zeta, L; t)$ in (3.54a) are decoupled for $m \neq n$ and diffuse separately with respect to L [71]. If $\bar{f}(\zeta, x, L; t)$ is initially in its lowest pitch-angle eigenmode $g_0(x)$, therefore, it will continue in this eigenmode and diffuse according to (3.50) as time goes on. On the other hand, off-diagonal elements of \bar{D}_{LL}^{mn} , which are obviously substantial in radial diffusion caused by magnetic impulses (see Section III.2), serve to couple distinct pitch-angle eigenmodes and thereby "excite" modes not present in the initial configuration of $\bar{f}(\zeta, x, L; t)$.

Inner-Zone Protons. For particles that do *not* undergo significant pitch-angle diffusion, the fundamental radial-diffusion equation is (3.01). Very energetic ($E \geq 100$ MeV) inner-zone protons are believed to be in this category. The principal source for these particles is known as CRAND (see Section III.1): cosmic rays incident on the upper atmosphere eject high-energy neutrons that beta-decay with a mean life τ_n ($\sim 10^3$ sec) in their own rest frame. At low latitudes the vertical flux J_n of these "albedo" neutrons is believed to be given [72] by

$$J_n \approx 0.044 (E/1 \text{ MeV})^{-1.86} \text{ cm}^{-2} \text{ sec}^{-1} \text{ MeV}^{-1} \quad (3.55)$$

at the top of the atmosphere ($r=a+h$, cf. Sections II.2 and II.7). The presence of these decaying neutrons²⁹ requires that a proton source term [38]

$$S \approx (J_n/2\pi\gamma\tau_n p^2)\chi \quad (3.56a)$$

be added to the right-hand side of (3.01). The geometric injection coefficient χ for equatorially mirroring protons is estimated by the expression [73]

$$\chi \approx (2/\pi) \sin^{-1} [(a+h)/La]. \quad (3.56b)$$

The arcsine represents the half angle subtended by the earth's atmosphere at the site of proton injection (neutron decay) in a model centered-dipole field³⁰.

The inner-zone protons injected by CRAND lose energy to free and bound ionospheric electrons [cf. (2.04)] but gain energy from the secular decrease of B_0 [cf. (2.05)]. Both processes leave the equatorial pitch angle invariant. The energy gain is an adiabatic effect, and so is automatically included if the problem is posed in the invariant coordinates M , J , and Φ , *i.e.*, in the form that reduces to

$$\frac{\partial \bar{f}}{\partial t} = S + \frac{\partial}{\partial \Phi} \left[D_{\Phi\Phi} \frac{\partial \bar{f}}{\partial \Phi} \right]_{M,K} + \frac{(4\pi q^4/m_e)}{(2MB_m^3/m_p)^{1/2}} \left[\frac{\partial(C\bar{f})}{\partial M} \right]_{K,\Phi}, \quad (3.57a)$$

²⁹The mean free path of a 100-MeV neutron before beta decay is of the order of one astronomical unit. Decay within the magnetosphere therefore does not significantly deplete the flux of cosmic-ray-albedo neutrons.

³⁰For this derivation of S , it is assumed that the neutron flux is isotropic at the top of the atmosphere, so that the omnidirectional neutron flux $J_{2\pi}$ is twice the vertical flux J_n . The unidirectional neutron flux above the atmosphere remains $(1/2\pi)J_{2\pi}$ by Liouville's theorem (Section I.3), for gyrophase angles compatible with ejection from the atmosphere. The result is a gyrophase-averaged proton source $(d\bar{J}_\perp/dt)_n = (1/2\pi\gamma\tau_n)(\chi/2)J_{2\pi}$, *i.e.*, a source for $\bar{f} (= \bar{J}_\perp/p^2)$ given by (3.56).

where [cf. Section II.2]

$$C = \bar{N}_e [\gamma^2 - 1 - \gamma^2 \ln(\lambda_D m_e v / \hbar)] + \sum_i \bar{N}_i Z_i [\gamma^2 - 1 - \gamma^2 \ln[2 m_e c^2 (\gamma^2 - 1) / I_i]] \quad (3.57 \text{ b})$$

The mirror field B_m is given in terms of the invariant coordinate Φ by $B_m = (1/8\pi^3 a^6 y^2 B_0^2) |\Phi|^3$, and thus contains an explicit time dependence (that of B_0^{-2}). Expressed as functions of K^2 ($\equiv J^2/8m_0M$) and Φ , the drift-averaged atmospheric densities \bar{N}_j also vary with time. The drift shell corresponding to given values of K and Φ not only contracts temporally (since $\dot{B}_0/B_0 < 0$), but also moves laterally relative to the earth so as to remain concentric with the dipole axis³¹ (apart from the effects of magnetic anomalies, cf. Section III.7). A growing dipole-offset distance imparts an additional increase to \bar{N}_j with time for atmospheric constituents whose densities decrease with altitude.

The secular variation³² of B_0 on a time scale ~ 2000 yr prevents (3.57) from having a steady-state ($\partial \bar{f} / \partial t = 0$) solution with which the inner proton belt can be identified. Thus, the present state of protons in the inner zone is the result of a long and continuing process of evolution. According to Fig. 14 (Section II.2) protons presently trapped in the inner zone may well have resided there for the past thousand years or more. An integration of (3.57) over this geomagnetic history may be fraught with uncertainty, in view of the available observations. Such a treatment appears to be necessary, however.

In much of the inner zone, the secular decrease of B_0 energizes trapped protons more efficiently than does inward radial diffusion at constant M and J . Typical time scales for the latter process at $J=0$ have been indicated by broken lines in Fig. 14 (Section II.2). For this purpose, the diffusion "current" $-D_{LL}(\partial \bar{f} / \partial L)_{M,J}$ identified following (3.46) has been utilized to construct an effective "velocity"

$$\dot{L} = -D_{LL}(\partial \ln \bar{f} / \partial L)_{M,J} \quad (3.58)$$

Insertion of $10/L$ as a likely upper bound [38, 39] for $(\partial \ln \bar{f} / \partial L)_{M,J}$ leads to the estimate [cf. (2.05)] that

$$\frac{1}{E} \frac{dE}{dt} = \frac{\dot{L}}{B_e} \left[\frac{\gamma+1}{2\gamma} \right] \frac{\partial B_e}{\partial L} \approx \frac{30}{L^2} \left[\frac{\gamma+1}{2\gamma} \right] D_{LL} \quad (3.59)$$

³¹At present the distance between the dipole axis and the geocenter is growing at a rate ~ 2 km/yr.

³²Other axially symmetric internal multipoles (2^n) of odd- n order (e. g., octupole) may also contribute a significant secular variation having similar consequences [39].

if secular variation is neglected. The diffusion time scales shown in Fig. 14 (Section II.2) are obtained by inverting the right-hand side of (3.59) for representative values of D_{LL} at constant M and J (cf. Chapter V). These diffusion time scales are generally comparable to the secular and atmospheric time scales for e -folding the kinetic energy of an inner-belt proton having $M \sim 1$ GeV/gauss.

Other Diffusion Velocities. Since radial diffusion is a macroscopically random (rather than deterministic) process, it may be possible to identify "velocities" other than (3.58) by following the temporal evolution of \bar{f} in its various aspects. For example, the expansion of (3.01) as

$$\frac{\partial \bar{f}}{\partial t} - \frac{\partial D_{LL}}{\partial L} \left[\frac{\partial \bar{f}}{\partial L} \right]_{M,J} \approx L^2 D_{LL} \frac{\partial}{\partial L} \left[\frac{1}{L^2} \frac{\partial \bar{f}}{\partial L} \right]_{M,J} \quad (3.60)$$

suggests the inward motion (at "velocity" $-\partial D_{LL} / \partial L$) of a diffusing profile of \bar{f} , viewed at an "inflection point" where $\partial^2 \bar{f} / \partial (L^3)^2 = 0$. Alternatively, if the distribution function has a symmetrical "crest" shell at which $(\partial \bar{f} / \partial L)_{M,J} = (\partial^3 \bar{f} / \partial L^3)_{M,J} = 0$, this "crest" can easily be shown to move at "velocity"

$$\dot{L}_c = -2(\partial D_{LL} / \partial L) + (2/L) D_{LL} \quad (3.61)$$

when observed at fixed M and J . Finally, if (3.01) is recast as a Fokker-Planck equation [cf. (2.03)] of the form

$$\frac{\partial \bar{f}}{\partial t} = -L^2 \frac{\partial}{\partial L} \left[\frac{\bar{f}}{L^2} \frac{\partial D_{LL}}{\partial L} \right]_{M,J} + L^2 \frac{\partial}{\partial L} \left[\frac{1}{L^2} \frac{\partial (\bar{f} D_{LL})}{\partial L} \right]_{M,J} \quad (3.62)$$

the "velocity" $\partial D_{LL} / \partial L$ is seen to represent a mean displacement in L per unit time for the typical particle contained in $\bar{f}(M, J, L; t)$. Of course, in the presence of competing modes of diffusion the significance of such "velocities" is rather obscure. In general, the analysis of radiation-belt diffusion requires a complete application of the governing equations (see Chapter V). The direct identification of "diffusion velocities" from observations at fixed energy has enjoyed some historical popularity (see Section IV.6), but is no longer regarded as an adequate quantitative treatment of observational data.